AIAA 80-1165R

Combustion Wave Structures of High- and Low-Energy Double-Base Propellants

I. Aoki*
Nissan Motor Co., Ltd., Tokyo, Japan
and
N. Kubota†
Japan Defense Agency, Tokyo, Japan

This paper is concerned with the effect of the energy contained in double-base propellants on combustion wave structures and burning rate characteristics. The burning rates of high- and low-energy double-base propellants are shown as a function of NO_2 concentration at various pressures. The burning rate increases with increasing the weight fraction of NO_2 in the propellants and with increasing pressure. The reaction time in the dark zone decreased with increasing the pressure and energy level of the propellants. The heat flux transferred from the gas phase to the burning surface increases when the energy contained in the propellant is increased. Thus, the burning rate of a high-energy propellant is greater than that of a low-energy propellant.

Introduction

IN this study, the combustion wave structures of double-base propellants have been examined with the aim of extending their burning rate domain. While having the superior combustion characteristics of plateau burning and smokeless combustion products, double-base propellants also have, when compared to composite propellants, the undesirable characteristics of lower specific impulse and limited burning rate domain. For instance, the burning rate of composite propellants can be easily altered by changing the ammonium perchlorate particle sizes. This is not the case with double-base propellants where the burning rate can be increased by adding catalysts, such as lead stearate and lead salicylate, but not decreased by adding a suitable catalyst. Thus, double-base propellants operate in a very limited burning rate domain and it is difficult to achieve significantly higher or lower burning rates.

To increase the specific impulse of double-base propellants, oxidizers or high-energy materials such as ammonium perchlorate or HMX particles have been added. These propellants are called composite-modified double-base propellants. They demonstrate an increased specific impulse but no significant change to the double-base propellant burning rate domain. Therefore, a mechanism for increasing the burning rate domain of double-base propellants should also play an important role in extending the burning rate of a composite-modified double-base propellant. It is the purpose of this study to examine the combustion wave structure of a double-base propellant with the intent of extending the propellant's burning rate domain.

Combustion of Double-Base Propellant

In general, the burning rate of a double-base propellant increases with increasing pressure. This is because the gas phase reaction increases with increasing pressure and the heat feedback from this reaction zone to the burning surface of the propellant increases. Consequently, the increased heat in the gas phase increases the burning rate.

Extensive experimental and theoretical work has been performed in an effort to determine the decomposition and combustion processes of double-base propellants.[1-15] However, the details of the processes remain largely unknown, mainly because of the complexity of the chemical structure of double-base propellants. Generally, the primary ingredients in double-base propellants are nitrate esters. Typical nitrate esters are nitrocellulose (NC) and nitroglycerine (NG) which are mixed homogeneously with stabilizers. NC and NG have oxygen available in the form of $O\text{-}NO_2$ which is attached to certain organic molecules (e.g., cellulose). In the burning process, oxidizer from the nitrate group is released by thermal decomposition and reacts with other molecular decomposition products to produce heat.

The breaking of one $O\text{-}NO_2$ bond gives a free radical which decomposes to formaldehyde and nitrogen dioxide. The nitrogen dioxide exothermically oxidizes the aldehyde and other C-H-O species, producing nitric oxide. This reaction process occurs in the early stages of the gas phase reaction zone (fizz zone) and probably occurs in the solid phase and/or at the burning surface (condensed phase). The nitric oxide and other C-H-O species react in the gas phase above the burning surface (dark zone) and produce a high-temperature flame (luminous flame zone). Thus, the weight fraction of NO_2 in double-base propellants is responsible for the reaction rate in the gas phase and for the burning rate. These successive reaction zones are shown schematically in Fig. 1.

High- and Low-Energy Propellants

Since the energy contained per unit mass in a double-base propellant can be altered by changing the weight fraction of NO_2, propellants with varying energy content were formulated by using three methods: 1) changing the concentration of plasticizer at the constant mixture ratio of nitrocellulose and nitroglycerine, 2) changing the concentration of nitroglycerine, and 3) changing the concentration of nitrate group in nitrocellulose.

Twelve kinds of propellants were prepared by methods 1-3. The compositions of these propellants are shown in Table 1. The following calculated chemical and physical properties are shown in Table 1: weight fraction of NO_2 in the propellants, weight fraction of NO, heat of explosion, and final flame temperature. As shown in Table 1, propellants EC-1—EC-5 were made by method 1. The weight fraction of NO_2 in these

Presented as Paper 80-1165 at the AIAA/SAE/ASME 16th Joint Propulsion Conference, Hartford, Conn., June 30-July 2, 1980; submitted Sept. 12, 1980; revision received July 1, 1981.

*Research Engineer, Aeronautical and Space Division, (presently Visiting Engineer, Third Research Center, Technical Research and Development Institute, Japan Defense Agency). Member AIAA.

†Chief, Rocket Propulsion Laboratory, Third Research Center, Technical Research and Development Institute. Member AIAA.

Table 1 Specifications of all double-base propellant formulations[a] and chemical properties used for this study

Propellant	NC (N%)	NG	DEP	2NDPA	TA	W_{NO_2}	W_{NO}	H_{exp}	T_g
EC-1	53.0 (12.20)	40.5	4.0	2.5		0.466	0.304	1093	2756
EC-2	51.3 (12.20)	39.3	7.0	2.4		0.452	0.295	1005	2557
EC-3	50.2 (12.20)	38.4	9.0	2.4		0.442	0.288	944	2424
EC-4	48.0 (12.20)	36.7	13.0	2.3		0.422	0.275	825	2148
EC-5	45.8 (12.20)	35.0	17.0	2.2		0.403	0.263	706	1875
EC-6	43.6 (12.60)	42.8	10.5	3.1		0.447	0.292	953	2456
EC-7	43.6 (12.60)	39.9	13.4	3.1		0.430	0.282	850	2219
EC-8	43.6 (12.60)	37.0	16.3	3.1		0.412	0.269	747	1982
EC-9	43.6 (12.60)	34.1	19.2	3.1		0.394	0.257	644	1750
EC-10	60.0 (13.40)	25.0			15.0	0.416	0.271	886	2351
EC-11	60.0 (12.18)	25.0			15.0	0.392	0.256	790	2089
EC-12	60.0 (10.65)	25.0			15.0	0.365	0.238	664	1755

[a] NC = nitrocellulose NG = nitroglycerine DEP = diethylphthalate 2NDPA = 2-nitrodiphenylamine TA = triacetin W_{NO_2} = weight fraction of NO_2 in propellant W_{NO} = weight fraction of NO in propellant H_{exp} = heat of explosion, cal/g T_g = flame temperature, K

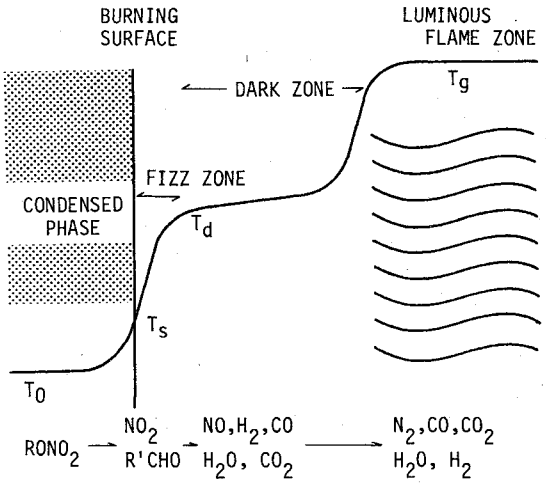

Fig. 1 Successive reaction zones of a typical double-base propellant.

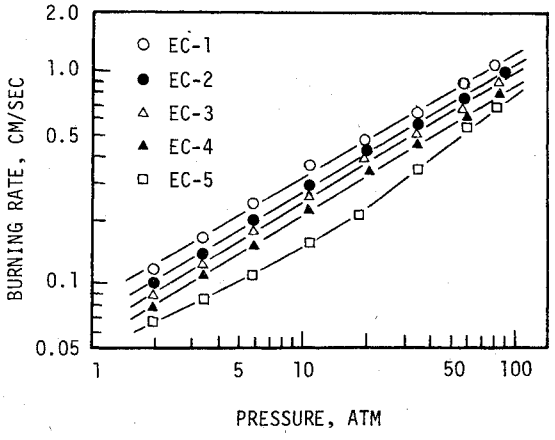

Fig. 2 Burning rates of the propellants made by method 1.

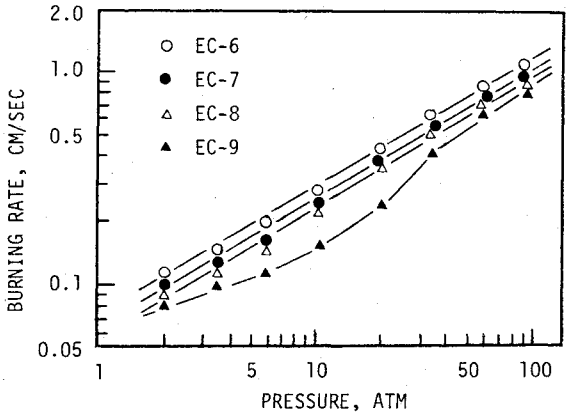

Fig. 3 Burning rates of the propellants made by method 2.

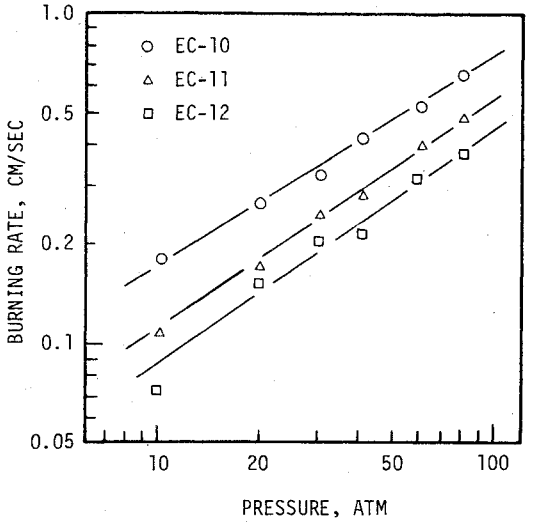

Fig. 4 Burning rates of the propellants made by method 3.

propellants, heat of explosion, and final flame temperature increase as the concentration of the diethylphthalate used as a plasticizer decreases. For example, the final temperature of propellant EC-1 is higher than that of propellant EC-5 by 881°C. For propellants EC-6—EC-9 which were made by method 2, the weight fraction of NO_2 in the propellants, heat of explosion, and final flame temperature increase as the concentration of nitroglycerine increases. The same is true for propellants EC-10—EC-12 which were made by method 3. For these propellants, the weight fraction of NO_2 in the propellants, heat of explosion, and final flame temperature all increase as the concentration of the nitrate group in the nitrocellulose increases.

The experimental investigations of the burning rate and the combustion wave were carried out using a chimney-type strand burner in which four transparent windows were mounted. Microphotographs of the gas phase and the burning surface of the propellants were obtained through the windows. The temperature profiles in the combustion wave were measured with fine thermocouples embedded in the propellant samples. These measurement techniques are described in Ref. 16.

Burning Rate Characteristics

The burning rates of propellants EC-1—EC-5, EC-6—EC-9, and EC-10—EC-12 are shown in Figs. 2-4, respectively. All

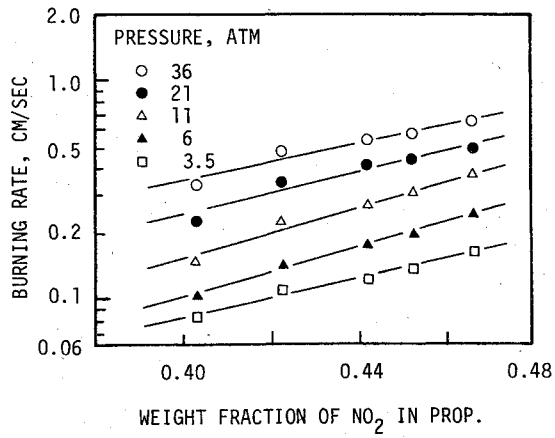

Fig. 5 Burning rate vs weight fraction of NO_2 in propellants EC-1—EC-5.

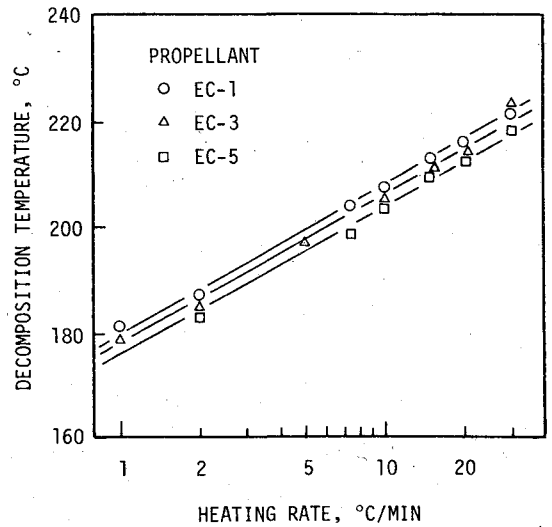

Fig. 6 Heating rate vs decomposition peak temperature.

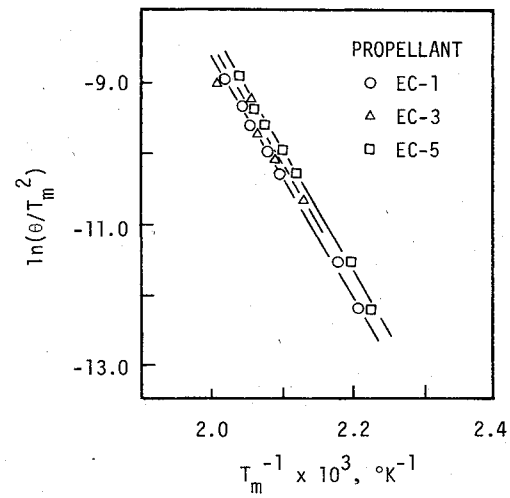

Fig. 7 Kissinger's plot for determination of activation energy.

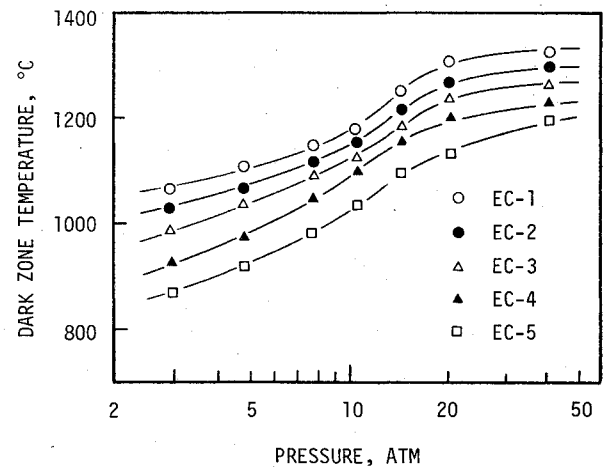

Fig. 8 Pressure vs dark zone temperature as a function of energy level.

of the burning rates increased linearly in log pressure vs log burning rate except for propellants EC-5 and EC-9, both of which were low-energy propellants. Also, Figs. 2-4 show that the burning rates of all the propellants increase as the energy content of the propellant increases.

Since the energy contained in the propellant is directly related to the weight fraction of NO_2 in the propellant, the burning rates of propellants EC-1—EC-5 shown in Fig. 2 were plotted as a function of the weight fraction of NO_2 in the propellant. As shown in Fig. 5, the burning rates increase as the weight fraction of NO_2 in the propellant increases. For example, the burning rate of the high-energy propellant EC-1 is approximately two times higher than that of the low-energy propellant EC-5. Since the burning rate increases linearly in the plot of weight fraction of NO_2 vs log burning rate, the relationship between the burning rates of these propellants and the weight fraction of NO_2 is represented by the following expression at a constant pressure:

$$r = a\exp\{b(NO_2)\}$$

where a and b are constants, r the burning rate, and (NO_2) the weight fraction of NO_2 in propellant. Since the burning rate increases linearly in the log pressure vs log burning rate plot, the burning rate is further represented by

$$r = \alpha\exp\{b(NO_2)\}p^m$$

where α is a constant which is dependent on the initial temperature of propellant, p the pressure, and m the pressure exponent of the burning rate. m and b for propellants EC-1—EC-4 were found to be 0.62 and 10.0, respectively.

Reaction in Condensed Phase

To understand the reaction mechanism in the condensed phase, the effect of the weight fraction of NO_2 on the condensed phase reaction was examined. A differential thermal analysis technique was used to determine the activation energies of the thermal decomposition process of the condensed phase. The heating rates of the propellant samples used in the analysis were 1-30°C/min in helium gas. The weight of the sample used was 1.1 mg in each measurement.

As shown in Fig. 6, the exothermic decomposition peak temperature increased when the heating rate increased (for propellants EC-1, EC-3, and EC-5). For example, the decomposition temperature went from 180°C at 1°C/min to 220°C at 30°C/min for propellant EC-1. While all of the data in this figure fall within the experimental scatter, it does appear that the higher energy propellants also had higher decomposition peak temperatures. The relationship between log (θ/T_m^2) and T_m^{-1} is plotted in accordance with the Kissinger's law in Fig. 7, where θ is the heating rate and T_m the decomposition peak temperature. The activation energies were found to be 33.6 ± 0.5 kcal/mole for all of the propellants tested in this study. Thus, no clear difference in the thermal decomposition characteristics between high- and low-energy propellants was observed within the range of heating rate tested in this study.

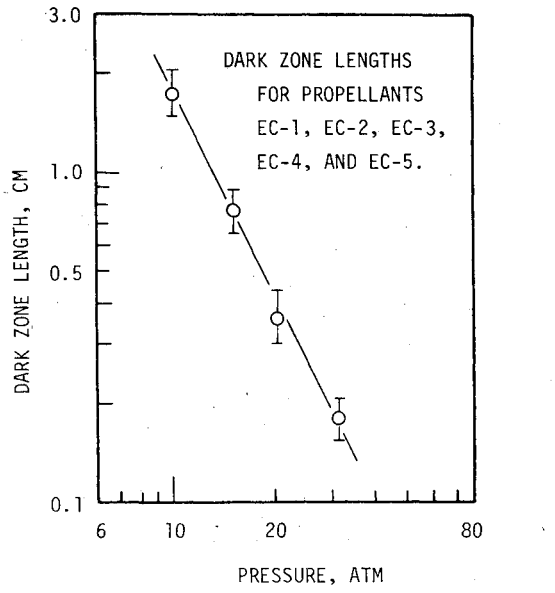

Fig. 9 Pressure vs dark zone length showing no clear dependence of dark zone length on propellant energy content.

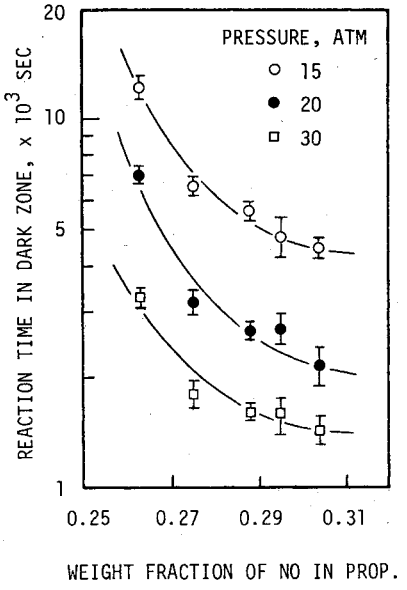

Fig. 10 Weight fraction of NO in propellant vs reaction time in the dark zone.

Reaction Mechanism in the Dark Zone

Since the final flame reaction to produce a luminous flame zone is initiated by the reaction in the dark zone, it is important to determine the reaction mechanism in the dark zone. The reaction time in the dark zone to produce the luminous flame zone was obtained from the measurement results of the dark zone length (the distance between the fizz zone and the luminous flame zone) and the burning rate of the propellant.

The reaction time in the dark zone is given by

$$\tau_d = L_d/u_d \tag{1}$$

where τ_d is the reaction time, L_d the dark zone length, and u_d the gas velocity in the dark zone. The velocity u_d is given by the mass balance equation between the gas phase and the condensed phase.

$$u_d = (\rho_p/\rho_d)r \tag{2}$$

where ρ_p is the propellant density and ρ_d the density in the dark zone. Using the equation of state and Eqs. (1) and (2), the following relationship for the reaction time in the dark zone is obtained:

$$\tau_d = pL_d/rR_d\rho_p T_d \tag{3}$$

where R_d is the gas constant in the dark zone and T_d the temperature in the dark zone.

In determining τ_d using Eq. (3), it is necessary to first determine the relationship between T_d and p, and L_d and p, in addition to r and p. The temperature measurement results in the dark zone obtained by fine thermocouples are shown in Fig. 8. Since the temperature in the dark zone increased with the distance above the burning surface as shown in Fig. 1, the T_d shown in Fig. 8 was determined as the temperature at the end of the fizz zone, which was equivalent to the temperature at the initial stage of the dark zone reaction. The T_d increased with pressure for pressures below about 20 atm, above which it became relatively pressure independent. Also, the T_d increased as the energy contained in the propellant increased for the pressure region between 3 and 40 atm tested in this study. However, the difference between dark zone temperatures in the high-energy propellant EC-1 and the low-energy propellant EC-5 was 200°C at most, which was much less than the final flame temperature difference of 881°C (see Table 1).

The dark zone length was measured by microphotographs at pressures between 2 and 30 atm. The dark zone lengths for all of the propellants tested were 2 cm at 10 atm and 0.2 cm at 30 atm. As shown in Fig. 9, no clear dependence of dark zone length on propellant energy content was seen. From Fig. 9, the dark zone length does appear to be dependent on pressure. When the pressure increases, the dark zone length decreases.

The reaction time τ_d was calculated using Eq. (3) and measured data r, T_d, and L_d. Since the determination of the gas constant R_d was rather difficult, it was assumed to be 34.0 kg·m/kg·°C for the propellant used in this study. As shown in Fig. 10, the reaction time in the dark zone was plotted as a function of the weight fraction of NO in the propellants because the reaction in the dark zone is reported to be directly related to the concentration of NO in the dark zone.[4-7] The τ_d decreased as the weight fraction of NO and pressure increased. However, the τ_d became less dependent on the weight fraction of NO as the weight fraction of NO increased. The reason is that the reaction rate in the dark zone is dependent on the mixture ratio of oxidizer and fuel species in the dark zone. The reaction rate becomes the maximum when the mixture ratio reaches its stoichiometric ratio. Thus, the τ_d approaches its minimum value as the weight fraction of NO increases, i.e., as the mixture ratio approaches its stoichiometric ratio.

It is known that the overall order of the reaction in the dark zone n to produce the luminous flame zone is represented by the following equation,[4,5]

$$L_d \sim p^{m-n} \sim p^d \tag{4}$$

where m is the pressure exponent of the burning rate (slope on a plot such as Fig. 2) and d the pressure exponent of the dark zone (slope on L_d plotted in Fig. 9). From Figs. 2 and 9, it is seen that m and d are fairly constant over a broad pressure range between 10 atm and 30 atm, except for the m of propellant EC-5. Thus, the overall order of the reaction is computed and determined to be 2.6 for all the propellants tested except EC-5. This suggests common chemical pathways in the dark zone are unchanged by changing the energy level of the propellant.

If one assumes a single-step reaction expressed as an Arrhenius type reacting in the dark zone, the activation energy in the dark zone can be obtained from the slope of the data plotted on a T_d^{-1} vs log τ_d^{-1} graph. Although the data

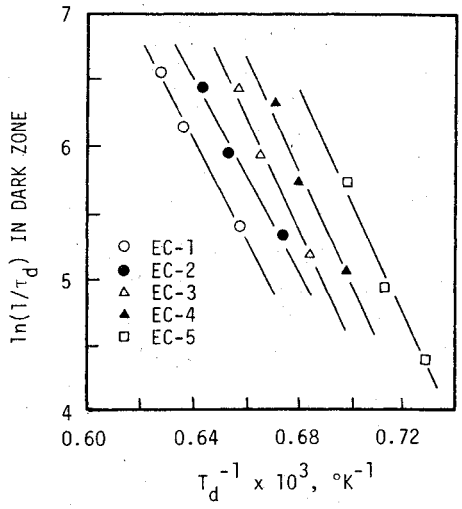

Fig. 11 T_d^{-1} **vs log** τ_d^{-1} **plot for determination of activation energy in the dark zone.**

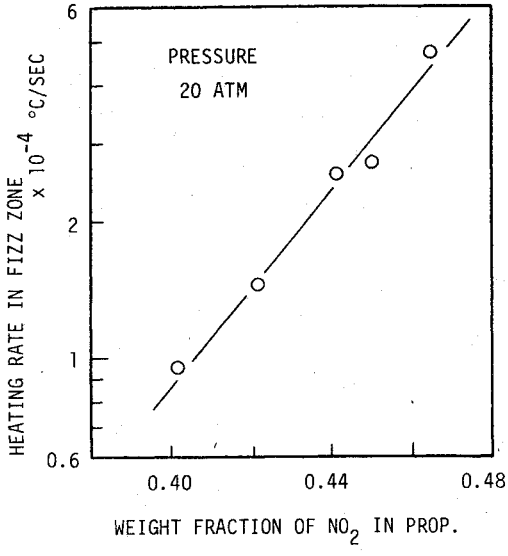

Fig. 12 Weight fraction of NO_2 vs heating rate in the fizz zone showing that the heating rate increases with the increasing weight fraction of NO_2.

shown in Fig. 11 were derived from scattered data of the measurement of the dark zone length and the temperature, the data shown in Fig. 11 yield straight lines and clearly differentiate the propellants. The activation energy was found to be 8.0±0.5 kcal/mole for propellants EC-1—EC-5. Again, this suggests that the common chemical pathways in the dark zone are unchanged by changing the energy contained in the propellant.

Reaction Mechanism in the Fizz Zone

Understanding of the fizz zone reaction mechanism is important because the burning rate of double-base propellants is controlled mainly by the reaction process in the fizz zone.[4,8,9,13] Thus, the experiments were conducted to determine the heat flux transferred from the fizz zone to the burning surface. The reaction time in the fizz zone is represented by

$$\tau_f = L_f/u_f \tag{5}$$

where τ_f is the reaction time in the fizz zone, L_f the fizz zone length, and u_f the gas velocity in the fizz zone. Since L_f cannot be measured by photographic observations as L_d was measured from the microphotographs, L_f was calculated

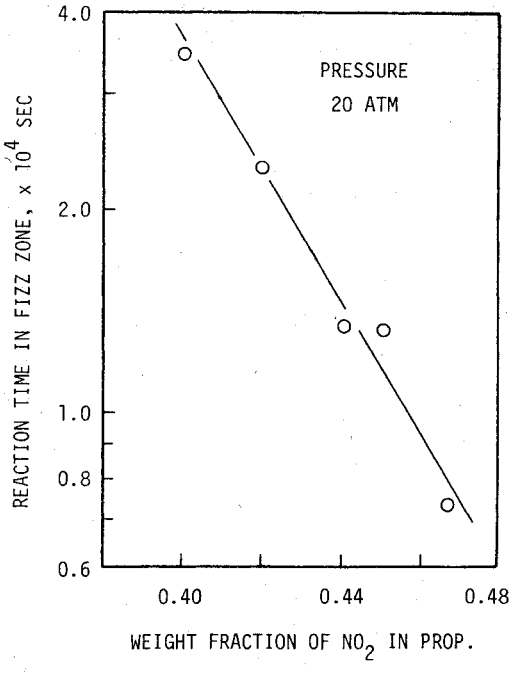

Fig. 13 Weight fraction of NO_2 vs reaction time in the fizz zone showing that the reaction time decreases with the increasing weight fraction of NO_2.

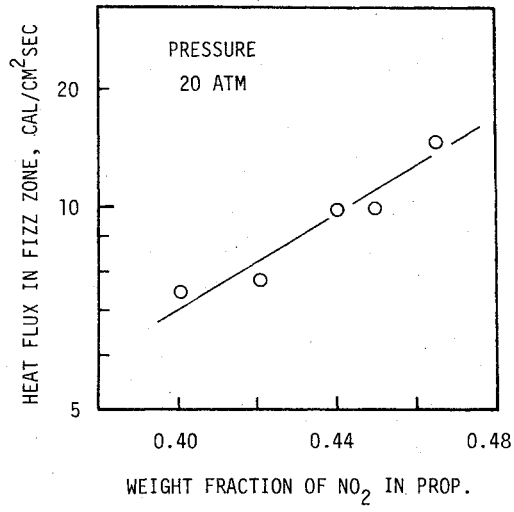

Fig. 14 Weight fraction of NO_2 vs heat flux from the gas phase to the burning surface showing that the heat flux increases with the increasing weight fraction of NO_2.

using the following

$$L_f = \frac{T_d - T_s}{(dT/dt)_f} r \tag{6}$$

where T_s is the burning surface temperature and $(dT/dt)_f$ the heating rate in the fizz zone.

Using the mass continuity equation and the equation of state in the fizz zone, the reaction time in the fizz zone is given by

$$\tau_f = \frac{T_d - T_s}{(dT/dt)_f} \frac{p}{\rho_p R_f T_f} \tag{7}$$

where T_f is the average temperature in the fizz zone given by $T_f = (T_d + T_s)/2$ and R_f the gas constant in the fizz zone. The

heating rate in the fizz zone was measured by microthermocouples which were embedded in the propellant samples. Since the reaction in the fizz zone is largely dependent on the reaction involving NO_2 reduction to NO, the heating rate was evaluated in terms of the weight fraction of NO_2. As shown in Fig. 12, the heating rate in the fizz zone increased with increasing pressure and with increasing weight fraction of NO_2.

The reaction time in the fizz zone was calculated using Eq. (7) and the data measured by the microthermocouples. The measured temperatures of the burning surface were rather scattered, however, ranging 295-323°C. No clear difference in T_s was obtained between high- and low-energy propellants. As shown in Fig. 13, the τ_f decreased with the increasing weight fraction of NO_2. For example, the τ_f of propellant EC-1 was 0.7×10^{-4} s, whereas for propellant EC-5 it was 3.5×10^{-4} s which is five times larger than that of propellant EC-1. This indicates the reaction time in the fizz zone decreases as the energy contained in the propellant increases.

If one assumes the heat conductivity in the fizz zone λ_f is equal to 1.5×10^{-4} cal/cm·s·°C, $\lambda_f(dT/dx)_f$ represents the heat flux from the gas phase to the burning surface of the propellant. Here $(dT/dx)_f$ is the temperature gradient in the fizz zone and x the distance. Figure 14 shows the relationship between the weight fraction of NO_2 and the heat flux. As shown in Fig. 14, the heat flux increased as the weight fraction of NO_2 increased at 20 atm. It also increased with increasing pressure (not shown in the figures). The heat flux of propellant EC-1 was 15 cal/cm^2·s and that of propellant EC-5 was 7.5 cal/cm^2·s, which is one-half of the heat flux of propellant EC-1 at 20 atm.

Since the heat flux from the gas phase to the burning surface is directly responsible for the burning rate of double-base propellants,[4,8,9,13] an increased heat flux in the fizz zone increases the burning rate of the propellants. Therefore, increasing heat flux with increasing the weight fraction of NO_2 in the propellant (i.e., high-energy propellant), increases the burning rate. It is evident from these results that the burning rate of high-energy propellants is higher than that of low-energy propellants because of the increased reaction rate in the fizz zone. Neither the reaction in the dark zone nor the reaction in the condensed phase is responsible for the burning rate when the energy contained in the propellant is changed.

Conclusions

The effect of the energy contained in double-base propellants on the combustion wave structure and the burning rate characteristics was examined experimentally. These results lead to the following conclusions. The burning rate increases with increasing the energy contained in the propellant, but the pressure exponent of the burning rate is less dependent on the energy level. The dark zone length, i.e., the luminous flame standoff distance, is very dependent on pressure but less dependent on the energy level. However, the reaction time in the dark zone decreased with increasing pressure and increasing energy level.

The reaction time in the fizz zone decreases with the increasing energy level of the propellant. The decreased reaction time increases the temperature gradient in the fizz zone. This increased temperature gradient increases the heat flux transferred from the gas phase to the burning surface of the propellant. Since the burning rate is nearly proportional to the heat flux, the burning rate increases as the energy contained in the propellant is increased.

References

[1] Crawford, B. L., Huggett, C., and McBrady, J. J., "The Mechanism of the Burning of Double-Base Propellants," *Journal of Physical and Colloid Chemistry,* Vol. 54, June 1950, pp. 854-862.

[2] Huggett, C., "Combustion of Solid Propellants," *Combustion Processes: High Speed Aerodynamics and Jet Propulsion Series,* Vol. 2, Princeton University Press, Princeton, N. J., 1956, pp. 514-574.

[3] Adams, G. K., "The Chemistry of Solid Propellant Combustion: Nitrate Ester or Double-Base Systems," *Proceedings of the Fourth Symposium on Naval Structural Mechanics,* Purdue University, Lafayette, Ind., April 1965, pp. 117-147.

[4] Kubota, N., Ohlemiller, T. J., Caveny, L. H., and Summerfield, M., "The Mechanism of Super-Rate Burning of Catalyzed Double Base Propellants," Rept. AMS 1087, Department of Aerospace and Mechanical Sciences, Princeton University, Princeton, N. J., March 1973.

[5] Kubota, N., Ohlemiller, T. J., Caveny, L. H., and Summerfield, M., "Site and Mode of Action of Platonizers in Double Base Propellants," *AIAA Journal,* Vol. 12, Dec. 1974, pp. 1709-1714.

[6] Sotter, J. G., "Chemical Kinetics of the Cordite Explosion Zone," *Tenth Symposium (International) on Combustion,* The Combustion Institute, Pittsburgh, Pa., 1965, pp. 1405-1411.

[7] Heller, C. A. and Gordon, A. S., "Structure of the Gas Phase Combustion Region of a Solid Double Base Propellant," *Journal of Physical Chemistry,* Vol. 59, Aug. 1955, pp. 773-777.

[8] Parr, R. G. and Crawford, B. L., "A Physical Theory of Burning of Double-Base Rocket Propellant," *Journal of Physical and Colloid Chemistry,* Vol. 54, June 1950, pp. 929-954.

[9] Rice, O. K. and Ginell, R., "Theory of Burning of Double-Base Rocket Propellants," *Journal of Physical and Colloid Chemistry,* Vol. 54, June 1950, pp. 885-916.

[10] Kubota, N., "Role of Additives in Combustion Waves and Effect on Stable Combustion Limit of Double-Base Propellants," *Propellants and Explosives,* Vol. 3, Dec. 1978, pp. 163-168.

[11] Lengelle, G., Duterque, J., Verdier, C., Bizot, A., and Trubert, J. F., "Combustion Mechanisms of Double Base Solid Propellants," *Seventeenth Symposium (International) on Combustion,* The Combustion Institute, Pittsburgh, Pa., 1979, pp. 1443-1451.

[12] Dauerman, L. and Tajima, Y. A., "Solid-Phase Reactions of a Double-Base Propellant," *AIAA Journal,* Vol. 6, April 1968, pp. 678-683.

[13] Kubota, N., "Determination of Plateau Burning Effect of Catalyzed Double-Base Propellant," *Seventeenth Symposium (International) on Combustion,* The Combustion Institute, Pittsburgh, Pa., 1979, pp. 1435-1441.

[14] Beckstead, M. W., "Model for Double-Base Propellant Combustion," *AIAA Journal,* Vol. 18, Aug. 1980, pp. 980-985.

[15] Cohen, N. S., "Analysis of Double-Base Propellant Combustion," AIAA Paper 81-0120, Jan. 1981.

[16] Sabadell, A. J., Wenograd, J., and Summerfield, M., "Measurement of Temperature Profiles through Solid Propellant Flames using Fine Thermocouples," *AIAA Journal,* Vol. 3, Sept. 1965, pp. 1580-1584.